FINAL REPORT

X-ray Studies of Highly Correlated Systems

Grant Number: DE-FG02-99ER45772
$300,000 granted from 6/1/2012 - 8/31/2017
Report DOE-WMU 45772

Principal Investigator:
Dr. Clement Burns
Professor of Physics
Western Michigan University
Dept. of Physics, Mail Stop 5252
Western Michigan University
Kalamazoo, MI 49008-5252
Phone: 269-387-4921
Fax: 269-387-4939
clement.burns@wmich.edu

Administration Contact:
Shellie Mosher
Office of Grants and Contracts
Western Michigan University
1903 W Michigan Ave
Kalamazoo MI 49008-5425
Office: (269) 387-4727
Fax: (269) 387-4737
shellie.mosher@wmich.edu

DOE OFFICE OF SCIENCE PROGRAM OFFICE:
BASIC ENERGY SCIENCE
X-ray Scattering

Program Manager:
Dr. Lane Wilson
Materials Sciences and Engineering Division
Office of Basic Energy Sciences
SC-22.2/Germantown Building, Rm F-411
U.S. Department of Energy
1000 Independence Avenue, SW
Washington, D.C. 20585-1290
Phone: (301) 903-5877
Fax: (301) 903-9513
Lane.Wilson@science.doe.gov

1. Abstract

The overall goal of the research was to improve the capabilities of x-ray synchrotron instrumentation to enable cutting-edge research in condensed matter physics. The main goal of the current grant cycle was to find a method to measure the polarization of the scattered x-ray in resonant inelastic x-ray scattering. To do this, we developed a polarization analysis apparatus using a thin, toroidally bent single crystal, which could be set to reflect one or the other of the two polarization components in the scattered x-ray beam. Resonant x-ray scattering measurements were also carried out on interfaces and the charge density wave in high temperature superconducting materials.

2. Introduction

X-ray synchrotron radiation from dedicated sources has provided a powerful research tool for condensed matter physics over many years. Over the past 18 years, we have been involved with DOE funded research to improve instrumentation for inelastic x-ray scattering, a technique which enables the study of excitations in materials with energies from 1 meV to several eV. This energy resolution makes it possible to study vibrational and electronic excitations in a wide variety of materials while varying parameters such as temperature and pressure. One of the main goals of the final grant period described here was the development of polarization analysis for the scattered x-ray for resonant inelastic x-ray scattering (RIXS). RIXS involves tuning the incident x-ray beam to the x-ray absorption edge of one of the atoms in a material, and often provides a strongly enhanced signal as compared to non-resonant scattering; the enhancement can be by factor of 100 or even more. Since inelastic scattering is very weak, it is often necessary to count for hours or days in order to get a good spectrum, so the signal enhancement from RIXS is critical. However, the theory of the RIXS process is much more complicated than for non-resonant inelastic scattering, which makes its interpretation more difficult. Polarization of the scattered x-rays provides a valuable piece of information to help with the interpretation of RIXS scattering. However, due to technical difficulties, the polarization is not easy to measure.

3.1 Development of Polarization Analysis for RIXS at the Iridium L_3-edge (Ref. [1])

Synchrotron sources provide a highly polarized incident x-ray beam, and so control of the incident polarization with respect to specific crystal axes can be achieved with proper sample orientation. For complete polarization analysis for RIXS we also need to analyze the polarization of the scattered photons. In RIXS, the photons are emitted at a variety of angles, and we need to collect a large solid angle while also carrying out high-resolution energy analysis in order to get sufficient signal. Diced, bent high quality single crystals such as Si or Ge, in conjunction with a position sensitive detector, are typically used to provide the energy discrimination.

Monochromatic, focused x-rays impinge on a sample at the center of the diffractometer. Scattered photons are diffracted from a diced, spherical, nearly perfect crystal analyzer; the diced crystal pieces are flat, resulting in a focal spot which is energy dispersive in the direction of the scattering plane of the analyzer. [3] The primary analyzer can be placed at a desired momentum transfer, Q, and the momentum resolution, ΔQ, is given by its solid angle acceptance. A position sensitive (strip-) detector is placed at the focal spot and measures the energy loss spectrum (see **Fig. 1a**). For polarization analysis, an additional crystal that can take the converging beam off the energy analyzer crystal and discriminate between the different polarization components is needed. The creation of such an element and the setup to enable its use was a main focus of this work. See **Fig. 1b** for the setup with polarization analysis.

For the polarization analyzer to work with the energy analyzer, we need it to provide a high efficiency Bragg reflection of the energy-analyzed and spherically focused photons and reimage them at the detector. For an analyzer with the revolution logarithmic spiral shape, the Bragg condition is satisfied for all x-rays diverging from a point source, but focusing becomes imperfect. [4] We developed curved optics which have a toroidal shape, designed to be a close approximation to a logarithmic spiral, but with

improved focusing characteristics which increase the energy resolution and efficiency. In earlier work, we made analyzers from curved graphite [4] for studies at the Cu *K*-edge (~8.980 keV), but these analyzers are not suitable for higher energy *L*-edges where much of the current interesting RIXS work takes place. Recently it has been shown that RIXS at the iridium L_3-edge can provide interesting information both about the electronic structure[5]and the dispersion of magnetic excitations. [6]

One of the results of the current project was the creation of a polarization analyzer for RIXS at the Ir L_3-edge ~11.215 keV. The analyzer is a Si (444) single crystal bent to a double-concave (toroidal) shape. This analyzer works at a Bragg angle θ_B of ~45° meaning it can almost totally separate the two polarization components. The analyzer was made from thin (50 μm) bent Si crystal optics, using a new fabrication method as described in a recent paper. [1] Work on this project was carried out on the medium resolution inelastic x-ray scattering spectrometers on Sectors 9 and 30 at the Advanced Photon Source (APS) at Argonne National Laboratory.

To characterize the overall energy resolution broadening and overall efficiency of a polarization analyzer, one needs to measure the resolution function at the primary focus in front of polarization analyzer with the conventional RIXS setup, and the resolution function at the secondary focus after the polarization analyzer. The resolution function at the primary focus without polarization analysis system has an FWHM of 172 meV, shown in blue in **Fig.** 1c. The FWHM of the spectrum at the secondary focus with σ polarization configuration is 246 meV which broadens the primary focus by 43%. This is not too far from our Monte Carlo result predicted a 33% broadening, indicating good fabrication.

Overall efficiency can be estimated by the ratio of the integrated intensity at the secondary focus and the primary focus. The overall efficiency turned out to be 0.4% which is lower by over an order of magnitude than the theoretical value. More recent results using an etched crystal have resulted in an efficiency of ~1%. Considering that incoming RIXS signals at the Ir edge can have signals of hundreds of counts per second, this efficiency, while less than ideal, is high enough for operation.

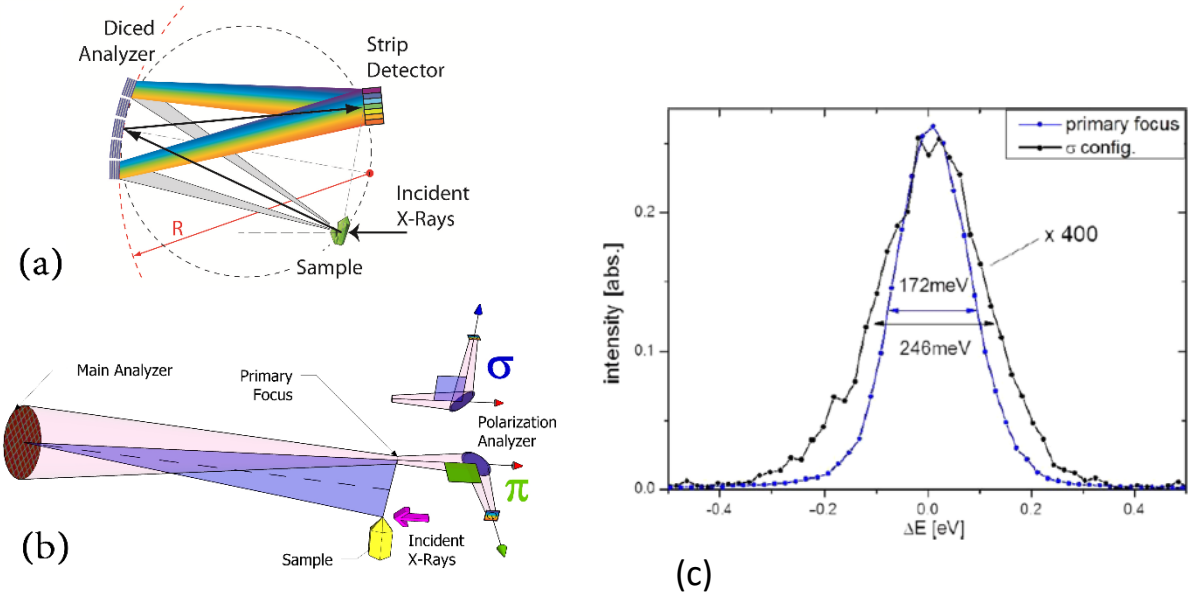

FIG. 1. (from Ref. [1]) (a) Rowland circle geometry showing the sample/analyzer/detector system. The rainbow at the strip detector illustrates the spread in energies from the flat, diced sections of the analyzer. (b) Refocusing scheme with polarization analyzer. The blue triangle plane represents the reflection plane of main analyzer. The blue rectangle plane represents the reflection plane of polarization analyzer, given the name σ in this configuration. The green plane is the π polarization component. (c) Energy resolution function at the primary focus before the polarization analyzer (blue curve) and secondary focus after polarization analyzer (black curve). Both spectra are taken with σ polarization of incident x-ray in the vertical diffraction geometry.

3.2 Polarization properties of synchrotron beam (Ref. [2])

We also studied the polarization properties of the synchrotron beam itself. While the x-ray beam in the plane of the synchrotron is linearly polarized with σ polarization, measurements which lie above or below the plane will also contain an incident π component. This π component provides a source which in principle can aid in alignment of the π-polarization setup for polarization analysis. In addition, since any sample has a finite size, there is some fraction of incident π polarized x-rays in any scattering measurement. Using the optics development beamline at Sector 1 of the APS, we carried out measurements above the plane of the synchrotron to measure this component as shown in **Fig. 2**. **Fig. 2a** shows the calculated and measured intensity of the synchrotron radiation above the plane of the synchrotron. **Fig. 2b** show the π (called P in this publication) component of the polarization as a function of position and angle above the beam. Calculations for both figures are based on a Monte Carlo ray tracing simulation as well as the equations for synchrotron radiation emission.

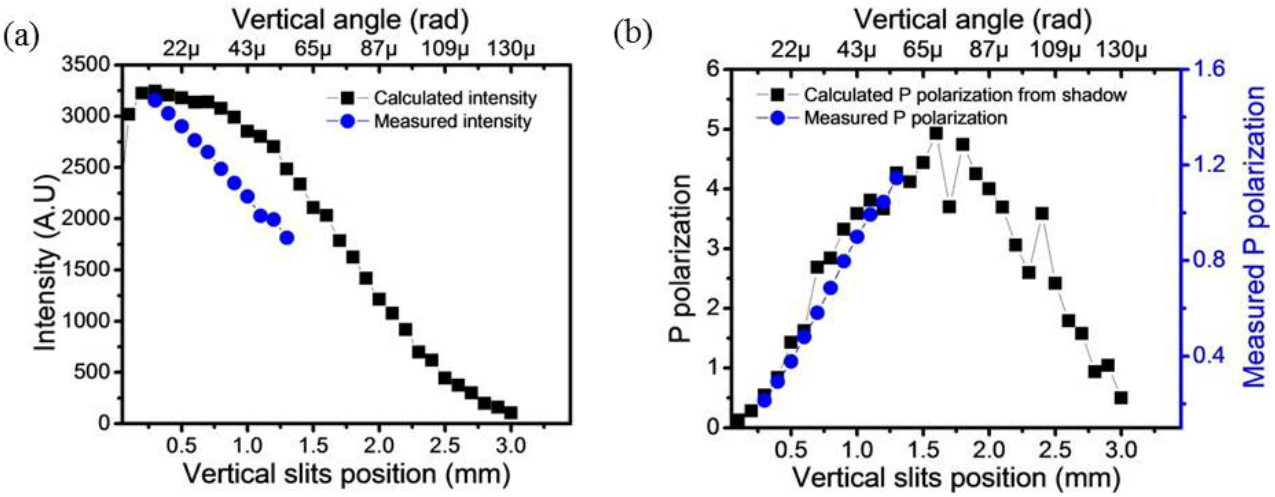

FIG. 2. (from Ref. [2]) Simulation (black squares) and experimental results (blue circles) of analyzer testing using a polarization setup at Sector 1-BM of the Advanced Photon Source. (a) Total intensity from the white beam slit and (b) scattered intensity of the P- polarization using polarization analyzer. Positions are referenced to the plane of the synchrotron

4.0 Research during sabbatical

From July 2015-June 2016, the PI was on sabbatical, working roughly half time with Dr. Jun-Sik Lee at the SLAC National Accelerator Laboratory on resonant x-ray scattering (RXS) studies of CDWs in cuprates. The other half of the sabbatical involved materials synthesis and transport measurements in the group of Dr. Ian Fisher in the Geballe Laboratory for Advanced Materials at Stanford University. This work was on lead chalcogenides, with interest in possible negative-U superconducting materials.

4.1 High field CDW in YBCO

Charge density waves are a well-established phenomenon in hole-doped cuprate superconductors (see for example [7-11]). Recently, it was discovered that in addition to the zero field 2D CDW, there is a high field CDW which has very long correlation lengths and three-dimensional type order [12]. During the recent sabbatical, the PI was part of the team that carried out more detailed measurements of the CDW at high fields, taking advantage of the high flux per pulse at the LCLS, and using a high field (up to 32 T) pulsed magnet [13]. Measurements were taken on high quality ortho-II and ortho-VIII $YBa_2Cu_3O_x$ (YBCO) single crystals, as a function of temperature and field. The 3D CDW was incommensurate with a very long in-plane correlation length (~100 lattice constants), and also a substantial correlation length between the planes (~10 lattice constants) as shown in **Fig. 3**.

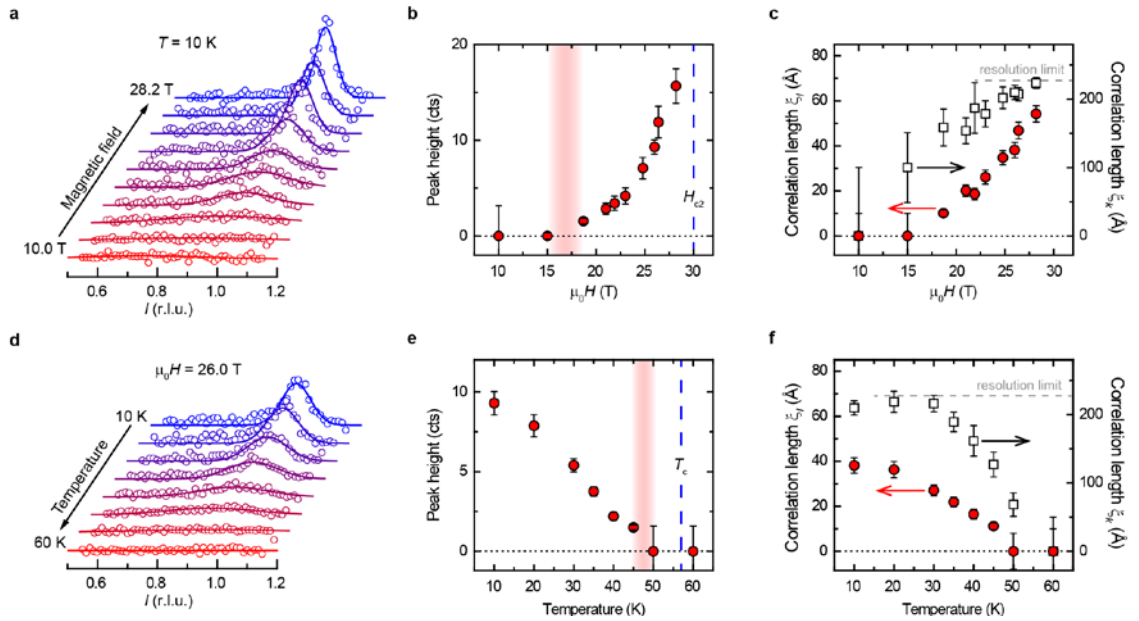

Fig. 3. (from Ref. [13]) CDW in YBCO ortho-II. The projected peak profile along (0, 1.67, *l*) as a function of magnetic field at T = 10 K(**a**) and as a function of temperature at $\mu_0 H$ = 26.0 T (**d**). Solid lines are Gaussian fits. **b, c,** Fitted 3D CDW peak heights (**b**) and correlation lengths (**c**) in the *l*- and *k*-directions as a function of $\mu_0 H$. **e, f,** Fitted 3D CDW peak heights (**e**) and correlation lengths (**f**) in the *l*- and *k*-directions as a function of temperature T. The red shaded area denotes the onset region of the 3D CDW. Dotted lines indicate zero and the error bars denote 1 standard deviation.

Both crystals show the formation of a 3D CDW at temperatures ~ 45 K, well below the 120 K of the quasi-2D CDW, which has a gradual onset near 120 K, and also below the superconducting transition temperature T_c ~ 60 K. The 3D CDWs in the two different samples also show an onset at a magnetic field of ~0.6 H_{c2}. These dependences indicate that the 3D CDW is in competition with superconductivity, and its formation is blocked without significant suppression of the superconductivity. Thus superconductivity wins out over the 3D CDW ground state at low fields.

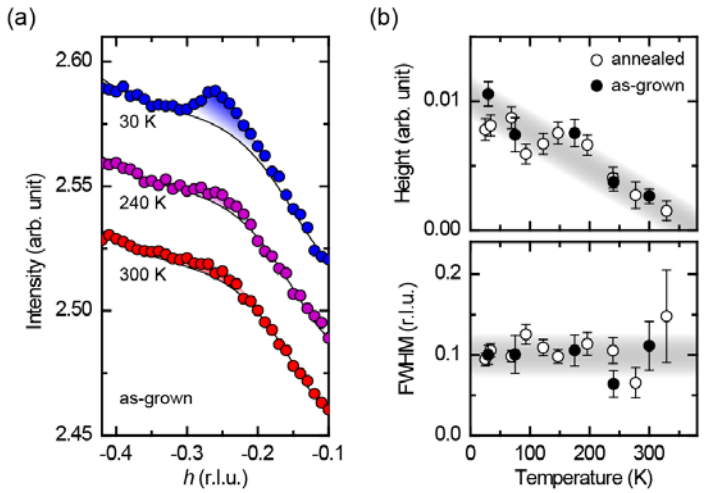

Fig. 4. (a) Temperature dependent *h*-scans in the as-grown NCCO (x = 0.14), measured at the Cu L_3-edge (931 eV). The colored shades denote the portion of peak above the background (black line) which was taken at T = 380 K. (b) Plots of height (upper) and FWHM (lower) of the peaks at $\boldsymbol{Q}_{CDW}$ as a function of temperature. The open and filled circles are from the annealed and as-grown NCCO, respectively.

4.2 CDW formation in electron-doped cuprates

The question arises whether CDW formation is ubiquitous in the cuprates or only found in the hole-doped systems. Resonant Soft X-ray Scattering (RSXS) measurements of the electron-doped cuprate $Nd_{2-x}Ce_xCuO_4$ (NCCO) for x = 0.14 and x = 0.15 at the Cu-L_3 edge by Neto et al. [14] showed broad scattering peaks, possibly indicative of CDW formation in the electron-doped cuprates. To gain further insight into the possibility of a CDW in the electron-doped cuprates, we carried out RSXS studies of electron-doped $Nd_{1.86}Ce_{0.14}CuO_4$ single crystals. As

grown, these materials are not superconducting, but become superconducting after annealing, which reduces the oxygen disorder. By studying annealed and unannealed materials, we are able to study the role of disorder on these materials.

X-ray scattering measurements in these systems show a clear peak above background as shown in **Fig. 4**, consistent with earlier work. There is no indication of a difference in the scattering between the superconducting and non-superconducting samples, so there is no indication of competition with superconductivity. In addition, incident energy dependent scans show additional features in the scattering, and a shift in the so-called CDW peak position with energy. This shift indicates either that 1) the scattering is NOT from a CDW, or 2) that there is significant other scattering (such as inelastic scattering) contributing to the peak as well as a CDW. Our conclusion is that the CDW like feature in this electron-doped cuprate is substantially different than the CDW found in the hole-doped materials.

5. Published papers with DOE support acknowledged – (Students, former students, and PI names in **bold**)

1) J. Park, B.-G. Cho, K. D. Kim, J. Koo, H. Jang, K.-T. Ko, J.-H. Park, K.-B. Lee, J.-Y. Kim, D. R. Lee, **C. A. Burns**, S. S. A. Seo and H. N. Lee, "Oxygen-Vacancy-Induced Orbital Reconstruction of Ti Ions at the Interface of $LaAlO_3/SrTiO_3$ Heterostructures: A Resonant Soft-X-Ray Scattering Study", Phys. Rev. Lett. 110, 017401 (2013).
2) Yu. V. Shvyd'ko, J. P. Hill, **C. A. Burns**, D. S. Coburn, B. Brajuskovic, D. Casa, K. Goetze, T. Gog, R. Khachatryan, J.-H. Kim, **C. N. Kodituwakku**, M. Ramanathan, T. Roberts, A. Said, H. Sinn, D. Shu, S. Stoupin, T. Toellner, M. Upton, M. Wieczorek, H. Yavas, "MERIX - next generation medium energy resolution inelastic x-ray scattering instrument at the APS", Journal of Electron Spectroscopy and Related Phenomena 188, 140 (2013).
3) Naresh Kujala, Albert Macrander, Xianbo Shi, Ruben Reininger, **Xuan Gao**, and **Clement Burns**, "Ray tracing simulation of 1-BM beamline at the Advanced Photon Source for polarization analysis of synchrotron optics", Proc. SPIE 9207, Advances in X-Ray/EUV Optics and Components IX, 92070F (2014).
4) **Xuan Gao**, Diego Casa, Jungho Kim, Thomas Gog, **Chengyang Li**, **Clement Burns**, "Toroidal Silicon Polarization Analyzer for Resonant Inelastic X-ray Scattering", Review of Scientific Instruments, 87, 083107 (2016).
5) H. Jang, B. Y. Kang, B. K. Cho, M. Hashimoto, D. Lu, **C. A. Burns**, C.-C. Kao, and J.-S. Lee, "Observation of orbital order in the half-filled 4f Gd compound GdB_4", Phys. Rev. Lett. 117, 216404 (2016).
6) H. Jang, W.-S. Lee, H. Nojiri, S. Matsuzawa, H. Yasumura, L. Nie, A. V. Maharaj, S. Gerber, Y. Liu, A. Mehta, **C. A. Burns**, D. A. Bonn, R. Liang, W. N. Hardy, Z. Islam, S. Song, J. Hastings, T. P. Devereaux, Z.-X. Shen, S. A. Kivelson, C.-C. Kao, D. Zhu, and J.-S. Lee, "Ideal charge density wave order in the high-field state of the YBCO superconductors", Proceedings of the National Academy of Sciences, 14645 (2016).
7) H. Jang, S. Asano, M. Fujita, M. Hashimoto, D. Lu, **C. A. Burns**, C.-C. Kao, and J.-S. Lee, "Superconductivity-insensitive order at $q \sim 1/4$ in electron doped cuprates", Physical Review X, in press.

6. Education and human Resources

Two graduate students, Xuan Gao and Chengyang Li, completed Ph.D. theses with research support from this grant. Dr. Gao's salary was paid by a funds from Argonne National Laboratory, but equipment and supply funds from the grant paid for all the materials used for his work. He is currently a scientist at the Chinese Academy of Science in Chongqing, China. Dr. Li's work was 100% supported by the grant. He is currently an instructor at the Southern University of Science and Technology in Shenzhen, China. A third graduate student, Gina Labriola, was supported for one summer under the grant but she transferred from the Ph. D. program in physics to the Masters' Program in Electrical and Computer Engineering. Three undergraduates carried out some work on equipment received under this grant, but their salary was not funded by the grant.

References Cited

[1] X. Gao, D. Casa, J. Kim, T. Gog, C. Li, C. Burns, Toroidal silicon polarization analyzer for resonant inelastic x-ray scattering, Review of Scientific Instruments 87 (2016) 083107.
[2] N. Kujala, A. Macrander, X. Shi, R. Reininger, X. Gao, C. Burns, Ray tracing simulation of 1-BM beamline at the Advanced Photon Source for polarization analyses of synchrotron optics, 2014, pp. 92070F-92070F-92076.
[3] S. Huotari, F. Albergamo, G. Vankó, R. Verbeni, G. Monaco, Resonant inelastic hard x-ray scattering with diced analyzer crystals and position-sensitive detectors, Review of Scientific Instruments 77 (2006) 053102.
[4] X. Gao, C. Burns, D. Casa, M. Upton, T. Gog, J. Kim, C. Li, Development of a graphite polarization analyzer for resonant inelastic x-ray scattering, Rev Sci Instrum 82 (2011) 113108.
[5] K. Ishii, I. Jarrige, M. Yoshida, K. Ikeuchi, J. Mizuki, K. Ohashi, T. Takayama, J. Matsuno, H. Takagi, Momentum-resolved electronic excitations in the Mott insulator Sr_2IrO_4 studied by resonant inelastic x-ray scattering, Physical Review B 83 (2011) 115121.
[6] J. Kim, D. Casa, M.H. Upton, T. Gog, Y.-J. Kim, J.F. Mitchell, M. van Veenendaal, M. Daghofer, J. van den Brink, G. Khaliullin, B.J. Kim, Magnetic Excitation Spectra of Sr_2IrO_4 Probed by Resonant Inelastic X-Ray Scattering: Establishing Links to Cuprate Superconductors, Physical Review Letters 108 (2012).
[7] J. Tranquada, B. Sternlieb, J. Axe, Y. Nakamura, S. Uchida, Evidence for stripe correlations of spins and holes in copper oxide superconductors, Nature 375 (1995) 561-563.
[8] C. Howald, H. Eisaki, N. Kaneko, A. Kapitulnik, Coexistence of periodic modulation of quasiparticle states and superconductivity in $Bi_2Sr_2CaCu_2O_{8+\delta}$, Proceedings of the National Academy of Sciences 100 (2003) 9705-9709.
[9] J. Chang, E. Blackburn, A.T. Holmes, N.B. Christensen, J. Larsen, J. Mesot, R. Liang, D.A. Bonn, W.N. Hardy, A. Watenphul, M.v. Zimmermann, E.M. Forgan, S.M. Hayden, Direct observation of competition between superconductivity and charge density wave order in $YBa_2Cu_3O_{6.67}$, Nat Phys 8 (2012) 871-876.
[10] E.H. da Silva Neto, P. Aynajian, A. Frano, R. Comin, E. Schierle, E. Weschke, A. Gyenis, J. Wen, J. Schneeloch, Z. Xu, Ubiquitous interplay between charge ordering and high-temperature superconductivity in cuprates, Science 343 (2014) 393-396.
[11] E. Blackburn, J. Chang, M. Hücker, A. Holmes, N.B. Christensen, R. Liang, D. Bonn, W. Hardy, U. Rütt, O. Gutowski, X-ray diffraction observations of a charge-density-wave order in superconducting ortho-II $YBa_2Cu_3O_{6.54}$ single crystals in zero magnetic field, Physical Review Letters 110 (2013) 137004.
[12] S. Gerber, H. Jang, H. Nojiri, S. Matsuzawa, H. Yasumura, D. Bonn, R. Liang, W. Hardy, Z. Islam, A. Mehta, Three-dimensional charge density wave order in $YBa_2Cu_3O_{6.67}$ at high magnetic fields, Science 350 (2015) 949-952.
[13] H. Jang, W.S. Lee, H. Nojiri, S. Matsuzawa, H. Yasumura, L. Nie, A.V. Maharaj, S. Gerber, Y.J. Liu, A. Mehta, D.A. Bonn, R. Liang, W.N. Hardy, C.A. Burns, Z. Islam, S. Song, J. Hastings, T.P. Devereaux, Z.X. Shen, S.A. Kivelson, C.C. Kao, D. Zhu, J.S. Lee, Ideal charge-density-wave order in the high-field state of superconducting YBCO, Proc. Natl. Acad. Sci. 113 (2016) 14645-14650.
[14] E.H. da Silva Neto, R. Comin, F. He, R. Sutarto, Y. Jiang, R.L. Greene, G.A. Sawatzky, A. Damascelli, Charge ordering in the electron-doped superconductor $Nd_{2-x}Ce_xCuO_4$, Science 347 (2015) 282-285.